KSTLE International Journal, Vol. 1, No. 1, June 2000, pp. 34-42

Wear Debris Analysis using the Color Pattern Recognition

Rae-Hyuk Chang[1]*, A.Y. Grigoriev[2], Eui-Sung Yoon[1], Hosung Kong[1] and Ki-Hong Kang[1]

[1]*Tribology Research Center, KIST, P.O. Box 131, Cheongryang, Seoul, 130-650, Korea*
[2]*Tribology Research Laboratory, MPRI, Gomel, Belarus*

Abstract : A method and results of classification of four different metallic wear debris were presented by using their color features. The color image of wear debris was used for the initial data, and the color properties of the debris were specified by *HSI* color model. Particles were characterized by a set of statistical features derived from the distribution of *HSI* color model components. The initial feature set was optimized by a principal component analysis, and multidimensional scaling procedure was used for the definition of a classification plane. It was found that five features, which include mean values of *H* and *S*, median *S*, skewness of distribution of *S* and *I*, allow to distinguish copper based alloys, red and dark iron oxides and steel particles. In this work, a method of probabilistic decision-making of class label assignment was proposed, which was based on the analysis of debris-coordinates distribution in the classification plane. The obtained results demonstrated a good availability for the automated wear particle analysis.

Key words: wear debris, classification, color features, multidimensional scaling, probabilistic recognition

Introduction

Wear debris analysis is one of the well known technologies for machine condition monitoring. It is because the peculiarities of machine elements interaction are well reflected in the process of particle generations and finally in their morphology. Thus, classification of wear debris in different morphological classes provides valuable information on the current state of wear occurred in machine systems.

In general, metallic wear debris is differentiated into several classes, e.g., rubbing, cutting, spherical, laminar, fatigue chunk and severe sliding wear particles. It has been recognized that each type has its own generation mechanism involving the specific wear process [1,2]. For instance, cutting wear particles are produced by the penetration, ploughing or cutting of one surface by another. Spherical particles are generated by cavitation erosion, welding and grinding processes [3,4]. The presence of severe sliding wear particles in a machine usually indicates a lubrication problem, as the consequence either of lubricant breakdown, or of unusually high loading.

In the discussed context, the morphology is mainly defined by shape, texture and color of wear debris. Normally, the wear particles are examined visually by an expert of considerable experience. However, break-through in computer and imaging technologies in these days makes automatic evaluation of the particle morphology possible. For different types of wear particles, their morphology may be characterized by a set of numerical features. Then, appropriate classification methods can be used for identifying particles into recognizable types [5].

*Corresponding author; Tel: 82-2-958-5664; Fax: 82-2-958-5659
E-mail: rhchang@kist.re.kr

Several numerous approaches for the automated particle classifications has been proposed for the quantitative description of particle morphology. But practically, all of the works have dealt only with the problems of shape and texture, not with those of color. The situation can be explained at least by two reasons. Firstly, the concept of color is basically qualitative. The color is not an absolute natural value since the persistence of color is formed by human eyes and brain.

Secondly, there were no cheap and accessible devices for color image acquisition. Usual way for exact color measurement is to estimate the light spectrum distribution and to use spectrophotometers. Only in the last decade, color CCD cameras became wide spread. In recent years, integration with appropriate hardware and software allows direct input of color images to the computer for analysis.

Color is an important feature in wear debris analysis [1, 6]. While the shape and texture features allow to differentiate metallic particle according to their prehistory of formation, the color allows to define the material depending on the properties of debris. The color directly related to the particle composition, so that it can be used for identification of corrosion product or wear severity in terms of particle temper color.

The composition of a sample particle extracted from the oil normally represents the materials of worn surfaces, contaminants and products of their chemical reaction initiated by water, heating and other reagents. At present, the objects are categorized by their color features in some broad groups: white metals, copper based alloys, red and black oxides. In oil lubricated conditions, such materials more often meet as steel, copper, lead, tin, chromium, silver and titanium. Ferrous oxides are usually divided into two groups: red or black oxides. As a result, this categorization allows to define the source of particle generation, lubrication condition, severity of wear

process and the presence of contamination in a lubricant, which consequently provide valuable diagnostic information on the current state of machinery.

In this work, the problem of wear debris classification was solved by the color features of wear debris. Three wide groups of materials included steel, copper based alloys and iron oxides (red and dark). Because of some difficulties in exact color matching procedure, a method of tri-stimuli color characterization was used. For this purposes, color images of wear debris obtained with a CCD camera was used for the initial data. The method based on the calculation of statistical features was derived from the values of *HSI* model color specification. The multidimensional scaling procedure and probabilistic decision-making functions were used for the particle classification.

Basic Theory

Color Formation

Visible light is electromagnetic radiation in the wavelength range of 400 nm to 700 nm. Color is the perceptual sensation of electromagnetic wave spectral distribution of visible light incident upon the retina of a human visual system. It must be mentioned that color is not a natural property of an object and perception of color only exists in the human eye and brain. From this point of view, the color sensation is constrained to the character of spectral distribution of visible light.

The physical production of color requires a source of light, exposed object and eye or some other type detectors. The electromagnetic radiance of light source is expressed by relative energy emitted at each wavelength and represented in the form of spectral power distribution (*SPD*), often in components each representing 5 or 10 nm band. The different sources have different shapes of the distribution. The *SPD* of daylight are presented in Fig. 1 (a).

When light interacts with an object, it transmitted, absorbed and reflected. The character of interaction is different according to the light wavelengths. For metals, the process can be described in terms of band theory of energy levels and efficiency of absorption and re-emission of photons. Then photons absorbed by electrons rise to a higher level of energy and re-emit the photon out of metal thus providing strong reflection of a polished metal. The efficiency of reflection depends on photon energy, so it is different for each metal. As a result, the reflected light is different from the source.

The effect of interaction of light with object is described by spectral reflectance or transmittance curves (*SRC, STC*), which characterizes the amplitude ratio of reflected/transmitted and primary light *SPD* on corresponded wavelengths. Fig. 1 (b) represents the spectral reflectance curves of typical industrial objects. It must be mentioned that in real cases there are other phenomena, which can contribute to the appearance of objects such as surface roughness, absorbed layers or fluorescence which results in variation of *SRC* (or *STC*) from the standard one.

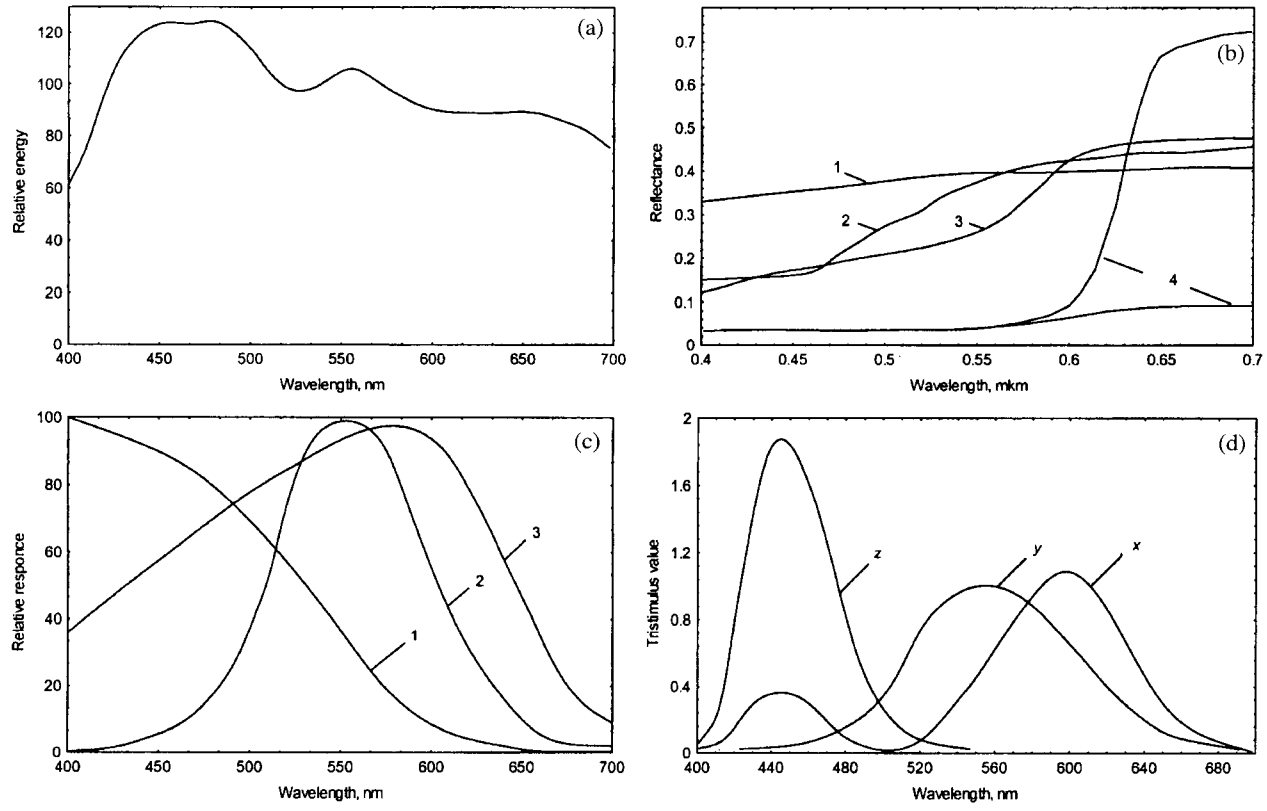

Fig. 1. (a) Spectral energy distribution of daylight; (b) Spectral reflectance curves of a set of typical metal products, 1 steel, 2 brass; 3 sheet copper, 4 iron oxides; (d) The spectral response curves 1 phototube, 2 eye, 3 photocell. All the data are qualitative.

The eye or other kind of detector is characterized by its response to the light of different wavelengths. The examples of spectral response function (*SRF*) of eye and some type of detectors are presented in Fig. 1 (c). So, the stimuli or *SPD* of light which form color perceptual sensation is expressed as

$$S = SPD_S \times SRC_O \times SRF_R \quad (1)$$

where S is *SPD* of stimuli; SPD_S spectral power distribution of light source; SRC_O spectral reflectance curve of an object; SRF_R spectral response curve of a recipient. The symbol $\times$ denotes element-by-element multiplication.

Color Measurement

For the technical applications, it is needed to have numerical measure of color. Spectral distributions of electromagnetic waves can be measured accurately by using photospectrometers, but for industrial applications the approach is not convenient. The current methods of color characterization are based on the fact that any colors can be specified in terms of three numbers representing the amount of the three primary lights added together [7]. In a qualitative form, it can be expressed as additive mixtures of 3 fixed primary colors.

The 3 color primaries can be chosen arbitrarily. Human retina also has three types of color photoreceptors: it is a logical choice to make them correspond approximately to the primaries of human visual system. As a result of color matching experiments, a standard set of such primaries has been specified by CIE(Commission Internationale de LEclairage). It consists of *X Y Z* primaries that correspond to colors of red, green and blue. The corresponded response functions $\bar{x}, \bar{y}, \bar{z}$ of human receptors are determined by measuring the mean color perception of a sample of human observers over a range of visible light. The response functions are shown in Fig. 1 (d). These curves specify how an *SPD* of stimuli can be transformed into a set of three numbers that specify a color. According to the approach, the quantitative measure of color is specified as a set of 3 numbers defined in equation (2)

$$X = \int_{\lambda} Q_{\lambda} \overset{\rho}{x}(\lambda) d\lambda \quad (2)$$

and similar for Y and Z. Here Q_l is defined as $SPD_S \times SRC_O$. The obtained values are usually normalized so that:

$$x + y + z = 1. \quad (3)$$

The resulted values of x, y, and z are considered as coordinates of 3 dimensional color space (color cube). One of the ways to represent all possible colors generated by mixing of primaries is chromaticity diagram, which shows color composition as a function of red (x) and green (y) (Fig. 2 (a)). For any value of x and y, the corresponded value of b is obtained from Eq.3.

Color Models

For specification of a color in some standard way, color models are used as follows. They are to introduce a transformation from 3D *XYZ* space into a new set of coordinates. Most of

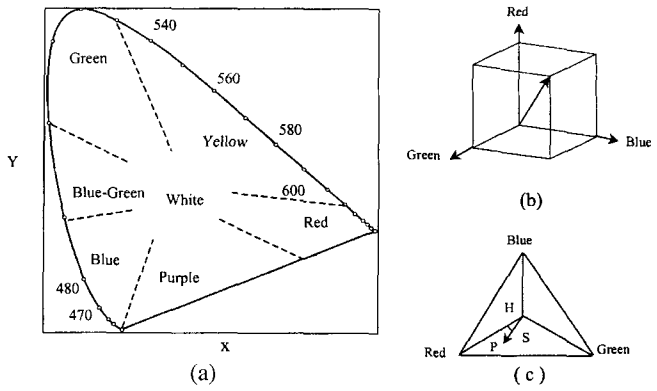

Fig. 2. (a) Chromaticity diagram and corresponded wavelength (the data is qualitative); (b) RGB color model scheme; (c) HSI color model scheme.

color models in use today are oriented either toward hardware or toward applications where the color manipulation is a main goal.

One of the commonly used for color image acquisition devices is *RGB* model. The model uses percentages of red, green and blue to create colors. Each component has levels of intensity, ranging from black to the component's full intensity. In computer graphic, the range is usually from 0 to 255 and each value of model components occupies one byte of memory. The graphical representation of the model is color cube shown in Fig. 2 (b). One of the advantages of the model is its simplicity in hardware realization and direct matching to the physical model of color formation and human vision. But the model is not fairly suitable for color manipulation because R, G, and B components incorporate chromatic and luminance values.

It was found that *HSI* model is more appropriate for the color manipulation. The *HSI* color model is based on the hue, saturation and, brightness components [8]. The color model is defined with respect to the color triangle (Fig. 2 (c)). The triangle vertices are defined by three initial colors. Hue is the color attribute that describes a pure color, whereas saturation gives a measure of degree to which a pure color diluted by white light. Therefore, the hue H of color point P is the angle of the vector shown with respect to the red axis. The saturation S of color point P is proportional to the distance from the center of triangle. The farther P is from the center of the triangle, the more saturated its color is. Intensity I in the *HSI* model is measured with respect to a line perpendicular to the triangle and passing through its center. While chromaticity and luminance components are separated, it allows simplifying some algorithms in image processing. That makes the *HSI* model handy tools in image processing.

Colors given in the *RGB* model can easily be converted to the values of *HSI* model. In the work, we used the following equations for converting incoming data from hardware to the *HSI* model for image processing [9]

$$I = \frac{1}{3}(R + G + B),$$

$$S = 255 - \frac{3}{(R+G+B)} min(R, G, B), \quad (4)$$

$$H = cos^{-1} \frac{0.5[(R-G)+(R-B)]}{\sqrt{[(R-G)^2+(R-B)(G-B)]}}.$$

Experimental Device

Fig. 3 represents an experimental device used for color image acquisition. The device consists of an optical microscope equipped by a single chip CCD color camera, a PC with peripherals and an image capture board. Additional color monitor was used for an auxiliary visualization device. The signal formed by CCD camera was put into PC via capture board. The specially developed software allows displaying image in PC monitor, capture and save it in one of the known image file formats for future analysis.

While the discussed device is assembled from general-purpose units, some technological consideration of the scheme is needed. The CCD cameras are constructed for converting optical image into video signal, which displayed into a monitor for observation. The human perceptual response to light intensity is highly nonlinear and can be expressed by the following function

$$I_h = I_o^{\gamma} \quad (6)$$

where I_o and I_h are original light intensity and response, γ is equal to 1/3. The cathode ray tube in monitors have almost nonlinear response for applied voltage of $\gamma = 5/2$. CCD cameras usually have linear response to light intensity and usually converted to obtain non-linearity of $\gamma = 2/5$. As a result of this, those images captured by CCD camera look naturally when observed on CRT. When absolute values of light intensities with a camera are measured, this non-linearity should be compensated with signal processing with $\gamma = 2½$. The presented scheme of video signal compensation is realized in the developed software for image processing.

The color data from CCD camera depends on lightening conditions. Voltage change of microscope illumination lamp leads to change of the source light *SPD* and the resulted color data (see Eq.1). To avoid the situation, the following calibration procedure was used. Lighting condition was tuned by matching images on display with a standard one. As the standard image was used, an image of rough copper surface with settings of acquisition device corresponded to the maximal visual matching displayed image when observed through microscopy oculars. The color balance of display was adjusted by Colorific technology. During the experiment, conditions of image acquisition was not changed.

Initial Data

Different kind of materials and real wear debris were used for the test samples in this study. The sample set of actual materials was used for reference points that compare their color properties to real wear debris. The set includes several

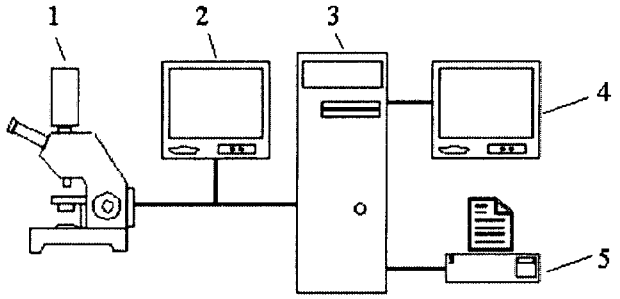

Fig. 3. General scheme of the wear debris image capture system: 1 optical microscope with CCD camera; 2 additional color monitor; 3 computer; 4 display; 5 color printer.

materials of machine elements and their corrosion products: copper alloys, medium carbon steel, iron oxide powder and collected from a surface of corroded steel surfaces.

Wear particles were obtained from the oil samples according to the standard procedure of wear debris analysis. The particles were deposited on the glass substrate by RPD(Rotary Particle Depositor) technique, flushed by drops of a solvent and dried. The collection of wear debris was corresponded to different stages of an equipment operation and included different types of debris verified by experts.

The objects were investigated in an optical microscopy in reflected white light. Color images were acquired using the device described above. The image format was 320×240 pixels with 24-bit color depth. From the images of wear debris and material surfaces, samples color textures were extracted. Each of the samples represented by a set of non-overlapped square sub-regions of 75 by 75 pixel size. Typical examples of particle images and extracted sub-regions are shown in Fig. 4.

Feature Extraction

It was assumed that material composition correlates to the values of *HSI* color space components. This assumption is rather general and does not contradict to the natural representation. As shown in preliminary investigations, the domains of *HSI* color space occupied by wear debris forms several common regions and there is no linear separability between debris of different types.

The situation of poor separability is well known in the field of pattern recognition and explained in terms of high correlation of primary features. The usual way to overcome the problem is to derive a set of secondary order features from the initial one, which aims at separating correlated and non-correlated feature's content. Unfortunately there is no theory for "good" feature selection and the problem is solved in the frame of traditional statistical approach. In the first stage, the sets of primary features are transformed into secondary one. The next is to investigate a new feature space and to optimize the corresponded feature space. The aim of the optimization is eliminating redundant features and to reduce dimensionality of the space. It leads to the simplifying of objects classification scheme and computational burden. The last stage is construction of decision-making rules, which allows classi-

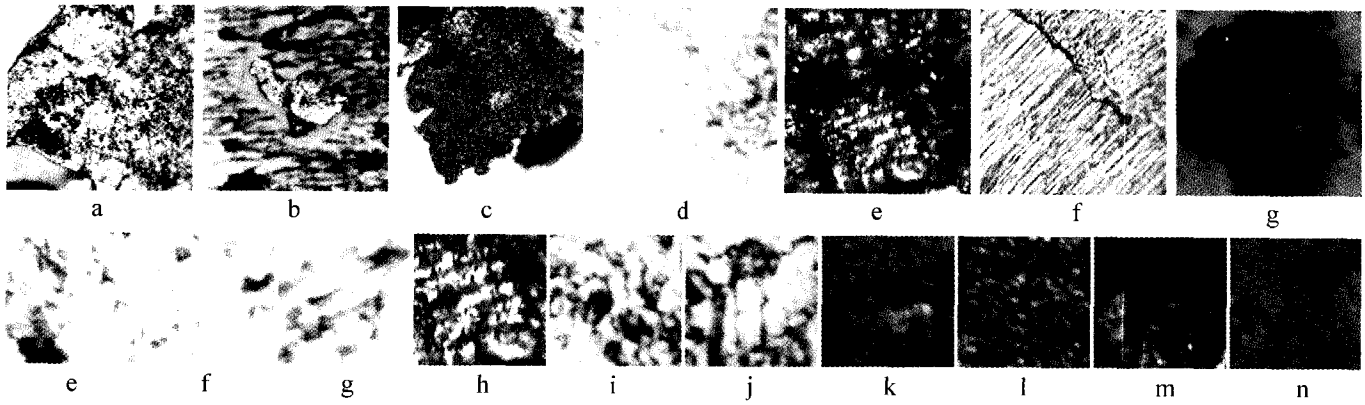

Fig. 4. Example of wear particles and surface of reference materials images (original images are in color). Wear particles: a -- steel; b -- copper alloy; c -- corroded steel particle. Textures of reference materials: d medium carbon steel; e -- bronze; f -- cooper; g - iron oxide powder; Images of subregions: e -- g steel; h -- j cooper and cooper based alloys; l -- n iron oxide;

fying the object to one of the classes by some superposition of secondary features. Thus, the problem of wear debris composition characterization is reduced to the definition of an appropriate feature set.

To derive the second order features from measurements of color properties of a wear debris image, histograms of *HSI* values distributions were represented. It is known that one of the simplest approaches for describing histogram is to use its moments [10]. If $h(x)$ is a histogram, the n^{th} moment of variable x about the means $\bar{x}$ is

$$\mu_n = \sum_i (x_i - \bar{x})^n p(x_i), \quad n > 1 \tag{7}$$

where $p(x_i)$ is probability of feature x_i. It was chosen moments up to the 4th order. Taking into account that location of occupied area of particles color features in the *HS* section of *HSI* space is directly correlated to their composition, the mean, median and geometrical mean of H and S values were also used in the feature set. The last statistics of I-values was not included to avoid some difficulties related to unequal lighting condition of captured images. As a result, the vector of 15 elements represents each of samples. To avoid influence of scale factor of features, they were normalized as:

$$x_i = \frac{x_i - \bar{x}}{\sigma^2}, \tag{8}$$

where σ^2 is standard deviation of feature, and x is calculated for samples analyzed test set.

The given feature set was optimized by a principal component analysis. The preliminary investigation of full-factor space was shown that more than 50% of feature variances are accounted by 2 factors only. According to that, two-factor space was selected for analysis and the corresponding feature loadings were calculated under varimax rotation strategy. The graph of the loadings is presented in Fig. 5 (a).

The graph analysis shows that the strong feature variation is observed along the both axes. This data can be interpreted in terms of linear separability of objects. With the loadings threshold of $T>0.75$ by screen test were extracted 5 most significant features (Fig. 5 (b)). The corresponded border on the factor plane is shown by the ellipse in Fig. 5 (a). The features are located on the longest distances from the factor plane origin. So, according to the obtained results, the initial feature set can be reduced up to the 5 features, which with high probability can form linear separable feature space of concerned objects.

Particle Classification

For investigation of feature space, the concept of the distance measure in the feature space is used. According to this concept, the features of the objects are considered as coordinates of some point in a multidimensional space. The distance between two points expresses the similarity of objects: if any points are close to each other, this indicates that there is a strong similarity between the corresponding objects. When the color features are used as coordinates, the location of a point depends on the peculiarity of the corresponding surface color properties, which are defined by material light reflectance ability and strongly relate to its native properties.

Furthermore, due to many factors such as surface roughness, the color of different points of the same objects varies in their values. For this reason, the objects of the same natures mapped in the feature space occupy some blurred domain cluster. The aim of investigation of color space is to define class borders, by which the objects can be divided into different clusters.

The most natural way of feature space analysis is visualization of cluster locations. But a human observer has difficulty in interpreting high-dimensional space on its original form. Direct visualization of more than 3 dimensional spaces is impossible. For overcoming the problem, we used a multidimensional scaling technique. The method allows mapping multidimensional data onto the reduced dimension space. Under this mapping, the inherent spatial structure of clusters is preserved as much as possible. This structure

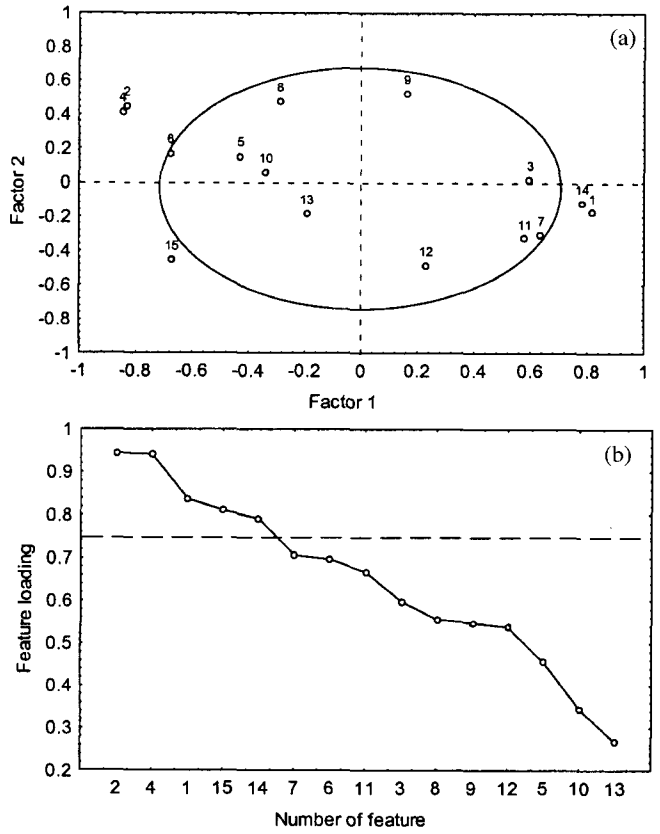

Fig. 5. (a) Factor loadings; (b) Screet test of factor loadings. 1, 2 mean, 3, 4 median; 5, 6 geometrical median of H and S values correspondingly; 7, 8, 9 standard deviation, 10, 11, 12 kurtosis; 13, 14, 15 skewness of H, S and V values of particle pixels correspondingly.

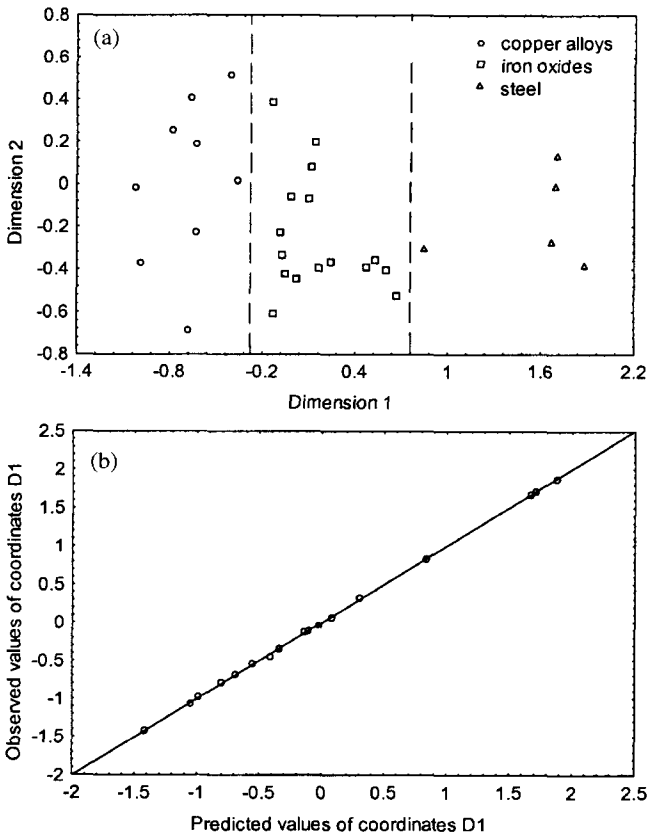

Fig. 6. (a) Classification plane of three types of wear particles; (b) The goodness of equation of axis D1 dimension fitting.

preservation is achieved by fitting mutual location of k points of *N*-dimensional space in *M* (*M*<*N*) dimensional one, such that their mutual distances from each other approximate the corresponding distances in *N*-space.

In common cases, the approach is based on a procedure, which rearrange objects around the space defined by a requested number of dimensions and checks how well the distances between objects in the space match the distances in the initial space. It is not an exact procedure and uses a function minimization algorithm that evaluates different configurations with the goal of maximizing the goodness of fit.

One of the approaches of measuring the distance in a multi-dimensional space is to use a *d*-dimensional Euclidean metric, an obvious generalization of two-dimensional distance:

$$e_{kl} = \left[\sum_{i=1}^{d} (x_{ik} - x_{il})^2 \right]^{1/2}, \qquad (9)$$

where e_{kl} is Euclidean distance in *d*-dimensional space; x_{ik}, x_{il} are the *i*-th components of feature vectors of *k* and *l* objects respectively. In order to evaluate how well a particular configuration reproduces the observed distances, the stress measure was used as follow,

$$\psi = \sum_{k=1}^{n-1} \sum_{l=k+1}^{n} (e^{(o)}_{kl} - e_{kl})^2 \qquad (10)$$

where $e^{(o)}_{kl}$, e_{kl} are observed distances and reproduced one respectively. There are different approaches for a multi-dimensional scaling procedure [11]. In the work, we used Shepard-Kruskal algorithm of the procedure [12]. The result of mapping initial 5-dimensional space onto the 2D one is shown in Fig. 6 (a).

Inter-class Separation

The obtained result shows good clustering for the initial 3 groups of objects along the axis of Dimension 1 (D1) into 3 categories: steel particles, corrosive and copper contained. The clusters have linear separability in the orthogonal direction of axis. The corresponded inter-class borders are showed on the plot.

For the analysis of a membership of any particle to one of classes from the initial feature space, it needs to be mapped on a classification plane. It is necessary to determine its dimensions for this purpose. For an analytical way of interpreting, the dimensions are to use multiple regression techniques to regress the features on the coordinates of the classification plane. As we have orthogonal linear separability of cluster along one axis (D1), it is possible for us to define the

dimension only that axis The equation of the axis dimension are defined by the linear regression as follows:

$$d = a_0 + \sum_{i}^{n} a f , , \{n = 1..5\} \quad (11)$$

The goodness of the fitting is estimated as the relative error of point location along the axis D1 and not exceeds 5% of their real location. The graph of observed values versus predicted is presented in Fig. 6 (b). Correlation of the data equals to 0.999 with 0 correlation between residual and observed values. So, the definition of D1 axis allows defining corresponded coordinate of any object.

The border of two linearly separable classes can be represented as

$$D_1 = d_1. \quad (12)$$

This line divides the entire space of a plane on two half-spaces with the corresponded classes. The decision making about a membership of a wear particle to one of classes ^{C} is reduced to check of the following condition

$$c = \begin{cases} 1 | d < D_{1-2} \\ 2 | d > D_{1-2} \end{cases} \quad (13)$$

where is the coordinate of inter-class border and is the coordinate of classified particle on corresponded axis. The given approach can be propagated for the n number of classes as follows:

$$c = i | D_{i-1,i} < d < D_{i,i+1}, i = 1.. n, D_{0,i} = -\infty, D_{n,n+1} = +\infty. \quad (14)$$

Intra-class Separation of Oxidized Particles

The result obtained above allows classifying analyzed particles into 3 classes that are initially formed in the test samples: copper based alloys, corroded and steel particles. In practice, the information on various type of steel and copper alloy particles is used for solving the problem of particle determination only. But in the case of corrosion-affected particles, it is possible to extract information about current condition of lubricant as well as severity of operation of controlled unit. The particles are classified into two subclasses red and black oxides. The first one is interpreted as the final reaction product of iron oxidation at room temperature. The black oxides are interpreted as a result of excessive heat during the particle generation.

The samples for the color textures of both types were added in the test samples. According to the graph of particles clustering presented above all, the particles are fallen into one group. Fig. 7 (a) showed a magnified part of oxidized particles domain of the graph. As it can be seen from the graph, the particles formed two partially overlapped clusters. The situation can be explained by the fact of significant variation of particle color. It is known that there are different forms of iron oxides varying in color in appearance, which can be extracted from oil [1]. Similar to the previous discussed approach, the interborder of classes can be defined as a line orthogonal to D1.

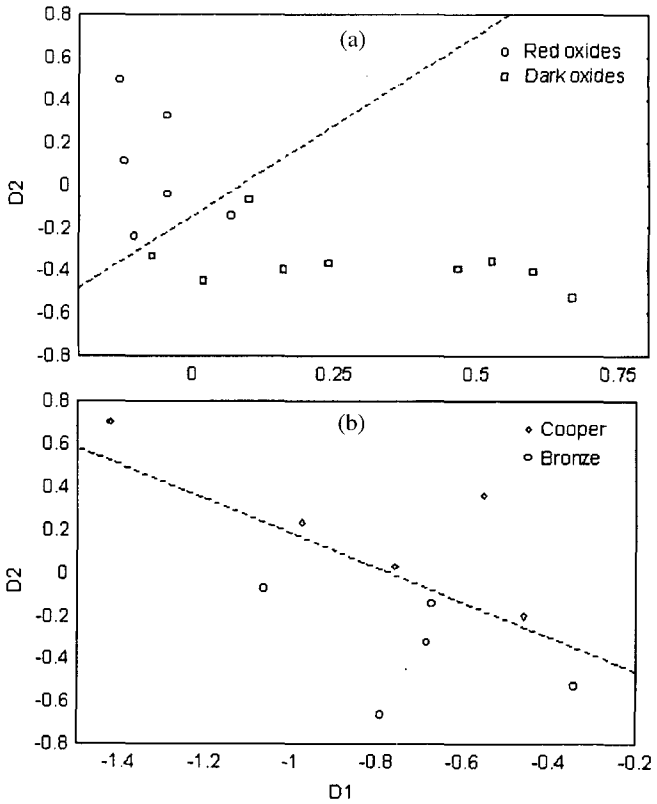

Fig. 7. Classification planes (a) of iron oxide particles; (b) cooper based alloys.

In the group of copper based particles, bronze debris was included. The part of classification plane of the class is presented in Fig. 7 (b). The particle of the class also can be devided into two groups along the axis dimension of D2. In that case, it is possible to define subclass border as a line orthogonal to D2. The corresponded borders are shown in the graphs.

Probabilistic Decision Making

The discussed above approach provides rigid classification, but it has some drawbacks related to impossibility to classify particles on the border of classes when $d = D_{i,i+1}$ or when classes are intersected. In addition it is not reflected location of classified object into class domain. It is clear that the object location expresses the relation degree to the class. Furthermore, it is rather optimistic to assume that the rigid inter-classes borders will be saved for real investigation. Due to many factors that lead to color variations, the particles of a class randomly spread in the class domain and can be located on the class borders. The objects located near the middle of a class domain have stronger degree of class relation; otherwise, it is less related.

For providing probabilistic recognition histograms of d, measure for each class of test sample was calculated. The histograms were fitted by the curves of normal low distribution. The obtained density functions are normalized by their maximum values to obtain probability data. The results

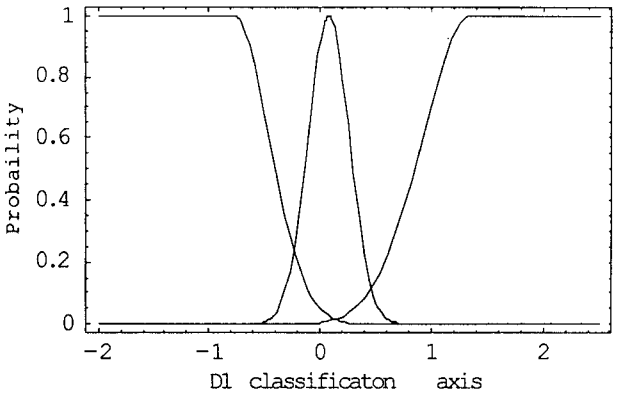

Fig. 8. Classification probabilistic functions of three types of particles along D1 axis

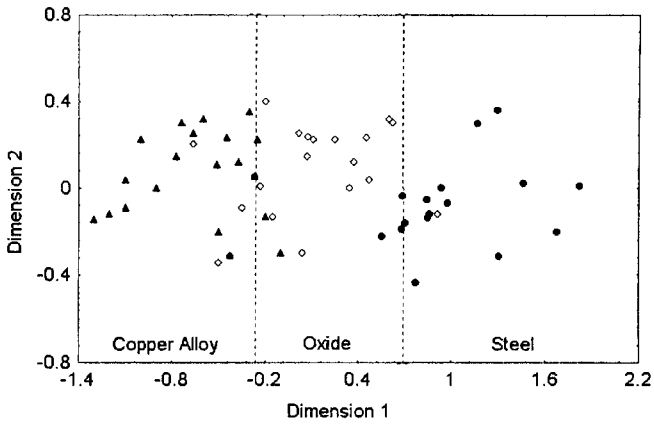

Fig. 9. Mapping results of sampled particles on classification plane of three types of wear particles.

are presented in Fig. 8 and illustrate the possibility of probabilistic classification of particles for copper-based alloys, iron oxides and steel materials. The decision making in probabilistic approach concludes in assigning to the analyzed particle class label corresponding to the curve with higher probability coordinate in the classification plane. The similar results can be obtained for intra-class differentiating of particles on copper/bronze and red/dark oxides correspondingly.

Results and Discussion

The presented data illustrate availability of wear debris estimation by color features. Since we did not use complex features and all of them are directly derived from the primary measurements, the method can be reproduced in other laboratories for other type of materials. As a result, it is possible to define some type of standard of wear debris composition map by accumulation all the data on one classification plane. The plane can be used as a standard reference map for wear debris identification.

The equation of linear transformation from standard code was obtained with the coordinate values of the standard reference map and 5 features using the multiple regression technique. Mapping of arbitrary sampled particles on the classification plan using this equation is shown in Fig. 9. In this mapping, most of sampled particles were mapped on its own category domain, but some were not. It may result from the problems related to the color measurement in realization.

As stated above exact color measurement, evaluation of spectral power distribution of reflected light is needed in some standard conditions. The realization of such a method for industrial application is not easy and cost-effective. For this reason, the method presented in the paper was based on commonly used hardware. One of the main drawbacks of the approach is that it would be difficult to reproduce obtained results on another set of hardware. Due to differences in lighting conditions, light optical paths and sensitivity of detectors, the final result would be different from obtained here. To overcome the problem, it is needed to use an appropriate calibration method.

The problem of calibration in color science is not easy because the color is not an absolute property and for its realization is needed to use color standards. The calibration of color usually involves definition of so-called color gamut of evaluated system. The gamut is characterized by its position in the color domain. The calibration procedure consists of the position matching of real device gamut with standard one.

The full description of calibration method is out of contents of this paper. But without development of such kind of procedure, it would be impossible to develop a robust and reliable method for wear debris color analysis that will share common results of investigation in science community.

Conclusion

This paper has reported a method and results of 4 types metallic wear debris classification using their color features. Statistical features derived from histogram of *HSI* color model was used for characterization particle color. Investigation of extracted feature space by factor analysis allowed defining an optimal feature set. Possibility of construction of a two-dimensional classification plane from high order feature set of the debris was demonstrated by a multidimensional scaling.

The study has shown that analyzed particles occupy separable domains in the classification plane. Five features include mean values of H and S, median S, skewness of distribution of S and I, that allow distinguishing copper based alloys, red and dark iron oxides and steel particles. In this work, a method of probabilistic decision-making of class label assignment was proposed that was based on the analysis of debris coordinates distribution in the classification plane.

The obtained results allow making conclusion about possibility and availability of using color features for automated wear debris analysis.

Acknowledgments

Support for this work by the Ministry of Science and Technology through the National Research Laboratory Program (1999-44) is gratefully acknowledged.

References

1. Anderson D. W., Wear particle atlas, Report No NAEC-92-163, 1992.
2. Hunt T. M., Handbook of wear debris analysis and particle detection in liquids, Elsevier Applied Science, London, 1983.
3. Scott D., Mills G. H. Spherical Debris Its Occurrence? Formation and Significance in Rolling Contact Fatique, Wear 24, pp. 235-242, 1973.
4. Kwon O. K., Spherical particles formation in lubricated sliding contact, Journal of Friction and Wear 1 , No.17, pp. 51-59, 1996.
5. Thomas A. D. H., Davies T. and Luxmoore A. R., Computer image analysis and identification of wear particles, Wear 142, pp. 213-226, 1991.
6. Barwell F. T., Bowen T. P. and Westcott V. C., The use of Temper Colors in Ferrography, Wear 44, pp. 235-242, 1973.
7. Grassman H. Zur., Theorie der Farbenmishung. Ann. der Physik and Chemie, pp. 69-84, 1853.
8. Foley J. D., Van Dam A., Feiner S., Hugges J. and Philips R., Computer Graphics: principle and Practice, Addison Wesley Pub. Co., 1996.
9. Gonzalez R. C., Woods R. E. Digital Image Processing, NY: Addison-Wesley, 1992.
10. Mills F., Statistical Methods, NY:Columbia University, 1995.
11. Cox T. F., Multidimensional Scaling, Newcastle: Univ. of Newcastle, 1994.
12. Young F. W. and Torgerson W. S. TORSA, A Fortran IV program for Shepard-Kruskal Multidimensional Scaling Analysis, Behav. Science, Vol. 12, 1967.
13. Raehyuk Chang, Eui-Sung Yoon, Hosung Kong and A. Ya. Grigoriev., A study on automatic wear debris recognition by using particle feature extraction, KSTLE, Vol. 15, No. 2, pp. 206-211, 1999.